Self-Consistent Molecular Theory of Polymers in Melts and Solutions

Lucian Livadaru[†] and Andriy Kovalenko*[,†,‡]

National Institute for Nanotechnology, National Research Council of Canada, W6-010, ECERF Building, 9107-116 Street, Edmonton, AB, Canada, T6G 2V4, and Department of Mechanical Engineering, University of Alberta, Edmonton, AB, Canada

Received: November 23, 2004; In Final Form: April 5, 2005

We propose a self-consistent molecular theory of conformational properties of flexible polymers in melts and solutions. The method employs the polymer reference interaction site model for the intermolecular correlations and the Green function technique for the intramolecular correlations. We demonstrate this method on *n*-alkane molecules in different environments: water, hexane, and in melt, corresponding to poor, good, and θ condition, respectively. The numerical results of the intramolecular correlation function, the radius of gyration, and the characteristic ratio of a polymer chain are indicative of conformational changes from one environment to another and are in agreement with other findings in the literature. Scaling laws for the chain size with respect to the number of monomers are discussed. We show results for the intra- and intermolecular correlation functions and the medium-induced potential. We also extract the Kuhn length and the characteristic ratio for the infinite chain limit for melts. The latter is compared to the experimental results and computer simulation. The conformational free energy per monomer in different solvents is calculated. Our treatment can be generalized readily to other polymer−solvent systems, for example, those containing branched copolymers and polar solvents.

1. Introduction

Since its initial proposal, the reference interaction site model (RISM)[1,2] has been proven to be a valuable tool for the study of molecular liquids. Its merits were soon thereafter exploited for determining the properties of chain molecules by means of the polymer reference interaction site model (PRISM)[3] designed for the study of various polymer systems, such as solutions, melts, and alloys. However, for practical purposes, in most cases the PRISM formalism requires to be supplemented with other theories or approximation schemes. This necessity emerges from the major difference in the conceptual treatments of the inter- and intramolecular correlations. For the latter, one often resorts to computer simulations for all but the simplest polymer models.

Self-consistent evaluation of the intra- and intermolecular correlations is a challenging task, and it often involves drastic approximations of the structure of the molecules involved. A variety of approximations have been proposed for intramolecular correlation, many of them based on simplistic models, such as the Gaussian chain, the freely rotating chain, and the wormlike chain.[30] They have the advantage of mimicking the chain flexibility and can, via adjustable parameters, be fitted to reproduce some of the experimental data. However, due to their oversimplified structure, these models cannot attempt to incorporate many of the structural details of molecules.

In their incipient PRISM work, Schweizer and Curro[3] studied the case of dense one-component polymer melts in the limiting case of Gaussian chains and rings with hard-core interactions. Subsequent work[4] tackled more realistic polymer models, such as ideal and nonoverlapping freely jointed chains, as well as extended the method to polymer blends.[5] A higher degree of chemical realism was implemented subsequently[6] by pursuing more complex models such as the semiflexible (wormlike) and rotational isomeric state (RIS) models. Melenkevitz et al.[7] utilized a variational approach for the limiting case of threadlike polymers as well as for the finite hard-core diameter model. The same authors utilized the density functional theory to derive an expression for the medium-induced potential,[8] which in turn can act as the coupling between intra- and intermolecular pair correlation functions. They combined the PRISM equation with Monte Carlo simulations to consider solutions of hard spheres. The work of Grayce et al.[9] exploited the concept of medium-induced potential to calculate the conformation of a single polymer modeled as a tangent-sphere freely jointed chain with Lennard−Jonnes (LJ) interactions by employing two methods (Monte Carlo simulation and the generating function) for the intramolecular correlation. Donley at al.[10] used the random walk model for which they were able to reduce PRISM to a set of coupled integral equations solved numerically. Other developments involved density functional theories,[11−15] the PRISM combined with Monte Carlo simulations,[16−18] and analytically tractable approximations of the structure factor.[19,20]

A drawback of the PRISM theories is that for a given model system the success of their prediction often depends on the particular closure and/or the solvent-induced potential type incorporated in the theory. Some of the theoretical studies on simple homopolymer model fluids[9,21] have shown that the use of different solvation potential types for a given system can lead to drastically different predictions on the conformational properties. Another issue transpiring from various applications[22,23] is to what extent the accuracy of a theory approximating the solute−solvent interaction by a sum of effective two-body solvation potentials can be maintained for a broad range of conditions in model systems. It still remains unclear to what degree unexpected predictions are attributable to deficiencies

* Corresponding author. E-mail: andriy.kovalenko@nrc.ca.
† National Research Council of Canada.
‡ University of Alberta.

10.1021/jp044654w CCC: $30.25 Published 2005 by the American Chemical Society
Published on Web 05/06/2005

in the model itself (oversimplifying) or to the various approximations in the theory. In this perspective, it would be of great benefit to know how the PRISM theory used in conjunction with various types of solvation potential would fare when applied to more realistic polymer model systems. Furthermore, because there is no universally successful closure for the PRISM equation, there is also a need to explore new types of closure for polymeric systems, as well as to improve the approximations accounting for the intramolecular solvent-mediated interactions.

Recently, we have proposed a new method to self-consistently determine the inter- and intramolecular correlations of polymeric systems.[24] The method is numerically efficient for calculating the properties of chemically realistic, flexible polymers in melts, solutions, and alloys. It combines the polymer's Green function for calculation of the intramolecular correlation with the PRISM formalism for the intermolecular correlations. The advantages of our method consist of its linear scalability with the polymer size and its ability to obtain bulk thermodynamics by analytical methods alone. It also avoids any statistical errors inherent in simulations.[25] In this paper, we present the theory in more detail and demonstrate it in the case of a homopolymer (polyethylene).

The paper is organized as follows. In the next section, we describe the molecular model and the approaches used for calculating the properties of the system. We then proceed to list the numerical results for simple homopolymers belonging to the *n*-alkane series. We choose simple examples of solvent/environment spanning three regimes of solvation: good, poor, and θ solvent. Our objective is the description of the conformational properties of the polymer (intramolecular distribution, radius is gyration, characteristic ratio), as well as the intermolecular correlation functions. The effect of solvent on the single chain properties is analyzed by comparison against the ideal chain case. Henceforth, by "ideal chain" we mean the phantom chain with the geometrical structure and local interactions of the real chain but no long-range interaction (therefore, no excluded volume or solvent-mediated interactions).

2. Model and Method

2.1. Polymer Model. To represent a polymer molecule, we chose the rotational isomeric state (RIS) model,[34] allowing us to incorporate the essential features of the polymer structure such as the bond length, b, the bond angle, γ, and the minima of the spectrum of torsional angles. It is a well-established fact that the potential energy terms associated with bond stretching and bond angle bending are much greater than those characterizing dihedral angle rotation. Therefore, we estimate that for the purpose of the present study ignoring the stretching and bending degrees of freedom is quite appropriate. Besides, this simplification greatly facilitates the computational treatments of such polymers.

Energetically, the model is characterized by its local chemistry, which in our model consists of local bond energies and interactions. In addition, the chain exhibits excluded volume interactions (modeled by a mean field) between monomers four bonds or more apart along the chain. Each chain monomer is modeled as a united atom interaction site (with the hydrogens being built in implicitly). The force-field parameters are provided by the DREIDING force field of Mayo et al.[27] with the exception of the rotational potential, which in addition to the standard torsional term, has a term accounting for the interactions between sites three bonds apart

$$E_{\varphi}(\varphi) = \frac{E_1}{2}(1 + \cos\varphi) + \frac{E_3}{2}(1 + \cos 3\varphi) \qquad (1)$$

The coefficient E_3 was taken from the DREIDING force field, whereas E_1 was fitted so that the gauche difference ($E_{\text{gauche}} - E_{\text{trans}}$) for the alkane molecule assumes the widely accepted value of k_BT at room temperature. The use of such a model is suitable particularly for simple homopolymers such as *n*-alkanes, as was found experimentally[28] and theoretically.[26,29,30]

2.2. Intermolecular Correlations. In this paper, we make use of the polymer RISM equation of Schweizer and Curro[3] that connects the intra- and intermolecular correlations for pairs of sites (α,β) for a homogeneous and isotropic system. In the Fourier space, this reads

$$\hat{h}_{\alpha\beta}(k) = \sum_{\mu\nu} \hat{\omega}_{\alpha\mu}(k)\hat{c}_{\mu\nu}(k)[\hat{\omega}_{\nu\beta}(k) + \rho_\nu \hat{h}_{\nu\beta}(k)] \qquad (2)$$

where $\hat{h}$ and $\hat{c}$ are the Fourier transforms of the total and direct correlation functions, respectively, ρ is the site density, and $\hat{\omega}$ is the Fourier transform of the intramolecular correlation.

To solve the PRISM integral equation, we use the closure proposed by Kovalenko and Hirata,[31] which was successfully applied to various phase transitions in complex liquids and mixtures[32]

$$g_{\alpha\beta}(r) = \begin{cases} \exp[\chi_{\alpha\beta}(r)] \text{ for } \chi_{\alpha\beta}(r) \le 0 \\ 1 + \chi_{\alpha\beta}(r) \text{ for } \chi_{\alpha\beta}(r) > 0 \end{cases} \qquad (3a)$$

$$\chi_{\alpha\beta}(r) = -\beta u_{\alpha\beta}(r) + h_{\alpha\beta}(r) - c_{\alpha\beta}(r) \qquad (3b)$$

where $g_{\alpha\beta}(r) = h_{\alpha\beta}(r) + 1$ is the pair distribution function, $u_{\alpha\beta}$ is the pair potential, and $\beta = 1/k_BT$ is the inverse temperature. This relation combines the advantages of two consecrated closures in a nontrivial manner: (i) the *mean spherical approximation* applied to high association peaks and critical tails, flipping to (ii) the *hypernetted chain* (HNC) closure in the core repulsion region, with the flipping being controlled by the sign of χ, as opposed to the value of the radius.

2.3. Intramolecular Correlations. The probability of a given conformation of a polymer molecule is the product of two Boltzmann factors corresponding to the bare intramolecular potential due to the sites belonging to the same polymer chain, and to a medium-induced potential (MIP)[7−9] due to sites on the other molecules in the system. To the level of the HNC approximation this potential can be expressed as

$$\beta W^{(\text{mip})}_{\alpha\beta}(r) = -\sum_{\mu\nu} c_{\alpha\mu}(r) * S_{\mu\nu}(r) * c_{\nu\beta}(r) \qquad (4)$$

where $S_{\mu\nu} = \omega_{\mu\nu} + \rho h_{\mu\nu}$ is the total site-density pair correlation function and "*" means convolution in the direct space. Alternative forms of this potential are known, such as the Percus−Yevick (PY) type expression

$$\beta W^{(\text{mip})}_{\alpha\beta}(r) = -\ln|1 + \sum_{\mu\nu} c_{\alpha\mu}(r) * S_{\mu\nu}(r) * c_{\nu\beta}(r)| \qquad (5)$$

as well as the Martynov-Sarkisov (MS) type expression

$$\beta W^{(\text{mip})}_{\alpha\beta}(r) = 1 - [1 + 2\sum_{\mu\nu} c_{\alpha\mu}(r) * S_{\mu\nu}(r) * c_{\nu\beta}(r)]^{1/2} \qquad (6)$$

The polymer is thus characterized by an intramolecular correlation that depends not only on the structure and the energetics of the molecule itself but also on its environment through the shape and strength of the medium-induced potential between the sites of the polymer.

For the intramolecular correlation function, we employ the polymer's propagator (or Green function) method,[33,34,38] which is an exact technique for carrying out the statistical mechanics of single polymer molecules. This method stems from an implementation of the transfer matrix technique (imported from the statistics of ferromagnetic systems) to polymer science.[30,39−42]

In the following, we consider only homopolymeric systems, therefore eliminating the need for site-type specification. We denote $\mathbf{r}_{0\mu}$ a set of judicially chosen coordinates necessary to completely describe the position and orientation of the polymer's site ($\mu = 0, 1,..., N$, with N being the number of monomers). Let $P_\mu(\mathbf{r}_{0\mu})$ be the conditional probability (the Green function) that site μ is at $\mathbf{r}_{0\mu}$, given that site 0 is at the origin. Similarly, we denote by $P^*_\mu(\mathbf{r}_{0\mu})$ the conjugated Green function that is the probability that site μ is at $\mathbf{r}_{0\mu}$, given that site N is at any location. The essence of the propagator method consists of evaluating the probability distribution functions $P_\mu(\mathbf{r}_{0\mu})$ and $P^*_\mu(\mathbf{r}_{0\mu})$ by solving their integral equations (with the appropriate boundary conditions)

$$P_{\mu+1}(\mathbf{r}_{0\mu+1}) = \int d\mathbf{r}_{0\mu} P_\mu(\mathbf{r}_{0\mu}) \mathbf{T}(\mathbf{r}_{0\mu},\mathbf{r}_{0\mu+1}) \quad (7)$$

$$P^*_{\mu+1}(\mathbf{r}_{0\mu+1}) = \int d\mathbf{r}_{0\mu} P^*_\mu(\mathbf{r}_{0\mu}) \mathbf{T}(\mathbf{r}_{0\mu},\mathbf{r}_{0\mu+1}) \quad (8)$$

where $\mathbf{T}$ is the transfer matrix accounting for the transfer probability between different states and for the effect of any existing external field, W. For a linear polymer, it can be written as a product of two factors

$$\mathbf{T}(\mathbf{r}_{0\mu}, \mathbf{r}_{0\mu+1}) = \mathbf{C}(\mathbf{r}_{0\mu},\mathbf{r}_{0\mu+1}) \exp(-\beta W(\mathbf{r}_{0\mu+1})) \quad (9)$$

where $\mathbf{C}$ is the connectivity matrix containing the statistical weights corresponding to "leaps" between the states of two adjacent sites. Generally, it can be calculated from geometrical considerations of the molecule alone.

The conformational partition function of a polymer can be calculated in this formalism by integration of the Green function corresponding to the end monomer[38]

$$Z = \int \mathbf{dr}\, P_N(\mathbf{r}) \quad (10)$$

from which the intramolecular free energy

$$A_{intra} = -k_B T \ln Z = -k_B T \ln \int \mathbf{dr}\, P_N(\mathbf{r}) \quad (11)$$

Within this formalism, the solvation free energy per unit volume is calculated as

$$A_{solv} = A_{inter} + N_p A_{intra} \quad (12)$$

where N_p is the concentration of the polymers and A_{inter} is the intermolecular free energy per unit volume obtained in the known form corresponding to the closure (eq 3a)[2,32]

$$\beta A_{inter} = -\frac{\rho^2}{2} \int \mathbf{dr} \sum_{\mu\nu} \left\{ \frac{1}{2} (h_{\mu\nu}(r))^2 \Theta(-h_{\mu\nu}(r)) - c_{\mu\nu}(r) \right\} + \frac{1}{2} \int \frac{\mathbf{dk}}{(2\pi)^3} \{ \mathrm{Tr}[\omega(k)\mathbf{c}(k)\rho] + \ln \det[\mathbf{1} - \omega(k)\mathbf{c}(k)\rho] \} \quad (13)$$

Because we are interested in the spatial distribution (correlations) of sites, $\mathbf{r}_{0\mu}$ must include the radial distance from the origin, $r_{0\mu}$. Knowledge of the Green function enables one to calculate the intramolecular correlation of a homopolymer (in the case when the site 0 is at the origin) by summing up the densities of all of the sites in the chain

$$\omega(r) = \delta(r) + c_0 \sum_{\mu=1,N} \int P_\mu(\mathbf{r}_{0\mu})\, \mathbf{T}(\mathbf{r}_{0\mu}, \mathbf{r}_{0,\,N-\mu}) P^*_{N-\mu}(\mathbf{r}_{0,\,N-\mu}) \quad (14)$$

where c_0 is a normalization constant. As a consequence, the finite length of the chain is reflected in the distribution, but the end effects are neglected.

The excluded volume interaction (the nonoverlap condition) can be represented by the following potential[38]

$$\beta W^{(ev)}(r) = v_0 \omega(r) \quad (15)$$

where

$$v_0 = \int \mathbf{dr} \{1 - \exp[-\beta u(r)]\} \quad (16)$$

is the excluded volume parameter.

The Green function method can directly account only for "local" interactions inside the molecular chain, such as the dihedral potential and the "pentane interaction" (the steric effect between monomers four bonds apart) and also for the interactions between the current site and the site situated at the origin (by current site we mean the site for which the Green function iteration is currently performed). Other interactions involving sites between the current and the zeroth site could be accounted, for instance, via an intramolecular mean field. In the context of our method, a useful mean field approximation between two given sites of a chain would incorporate the interactions mediated by all of the other sites of the chain, thus reducing the many-body interactions to an effective two-body potential. We propose a simple form (inspired by the Kirkwood approximation from the liquid state theory) for the intramolecular mean field due to the medium-induced interactions

$$\beta W^{(mf)}(|\mathbf{r}|) = \frac{\int \mathbf{dr}'\, \omega'(|\mathbf{r}'|)\, \omega'(|\mathbf{r} - \mathbf{r}'|)[W^{(mip)}(|\mathbf{r}'|) + W^{(mip)}(|\mathbf{r} - \mathbf{r}'|)]}{\int \mathbf{dr}'\, \omega'(|\mathbf{r}'|)\, \omega'(|\mathbf{r} - \mathbf{r}'|)} \quad (17)$$

where ω' is the intramolecular correlation function from which the self-correlation and the nearest neighbor terms with $\mu = 1-3$ are subtracted. This approximation is derived by placing site 0 at the origin, placing site μ at $\mathbf{r}$, and averaging the pair potentials over the positions of all of the other sites, irrespective of the orientational correlations between the spanned chain segments. The total potential "felt" by a polymer site, W, appearing in eq 9 is the sum of potentials u, $W^{(ev)}$, $W^{(mip)}$, and $W^{(mf)}$.

2.4. Numerical Methods of Calculation. Having established the coupling between the intra- and intermolecular correlations in the manner described above, the numerical task is to solve for both concomitantly. To obtain the intermolecular correlation function, we solve the PRISM equation by an iterative procedure carried out for the direct correlation functions, $c_{\alpha\beta}$, in real space via the method of modified direct inversion in the iterative subspace (MDIIS).[43] As described below in detail, each iteration step involves calculating the medium-induced potential by eqs 4−6, which is then used as an input for the Green function calculation of the intramolecular correlations. The iterations are repeated until self-consistency of both the intra- and intermolecular correlations is reached.

For the calculation of the polymer's Green functions, we first perform a transition from continuum to discrete coordinates. The coordinates in $\mathbf{r}_{0\mu}$, typically the radius and two rotational angles, all have finite ranges, which are divided into evenly spaced intervals. Thus, the integral equations in 7 and 8 are solved numerically by successive iterations starting with the initial condition.

The accuracy of the results of the Green functions for a given model is determined solely by the resolution of the mesh used in the numerical work. In the examples given in this paper, we ensured that the mesh resolution used for the intramolecular degrees of freedom is fine enough so that the accuracy of the conformational properties is better than ±10%. Note that it is increasingly costly to approach longer chains because the memory requirements increase linearly with the number of monomers. For more details on the Green function method and on the determination of the transfer matrix for various models, we direct the reader to the classical text of Flory[30] as well as to recent implementations of this technique.[26,33,34]

An iterative step of our computational method consists of the following algorithm (for simplicity, the Fourier transform operations are not mentioned):

(1) An initial guess is taken for the inter- and intramolecular correlations: initial ω is that of an ideal polymer (in the absence of any long-range interactions), whereas the initial c is the long-range part of the pair potential.

(2) The PRISM equation (2) is solved in k-space for the pair correlation function with the quantities determined in the previous step as an input.

(3) The medium-induced potential, W^{mip}, is calculated via one of the eqs (4−6). The intramolecular mean field (eq 17) is also derived from it.

(4) The intramolecular correlations in the presence of the MIP and the intramolecular mean field above are calculated by the Green function method.

(5) "Residuals" for the intermolecular correlation functions are determined as the difference between the pair correlation function, g, as calculated from the PRISM equation and g obtained from the closure relation. The residual for the intramolecular correlation is the difference between ω obtained just above and ω of the previous iteration step.

(6) The correlation functions and their residuals are processed by the MDIIS for minimizing the residuals; the optimized c and ω are used to start a new iteration step.

The self-consistency of the solution is achieved by concomitantly canceling the residuals constructed for both the inter- and intramolecular correlations.

For a polymer molecule in water, given the strong polar character of the environment, there can be very large variations of the inter- and intramolecular correlation functions at consecutive iteration steps. As a result, it is numerically difficult to reach the self-consistent solution simultaneously for the intra- and intermolecular correlations. Therefore, another procedure was implemented to obtain them separately. First, we fix the form of ω to be that corresponding to the ideal chain and solve the PRISM equation for the solute−solvent correlations. The latter then serve as an input to the self-consistent calculation of the medium-induced potential and ω for fixed intermolecular correlations. The two steps are repeated several times to reach a given iterative accuracy of the solution.

3. Results and Discussion

As we announced, the case study for our proposed method is a simple nonpolar flexible polymer structure: the *n*-alkane series. We consider polymers with various degrees of polymerization, up to about 200 monomers, in melt and in infinitely dilute solution. In the order of solvent quality for alkanes, the chosen environments rank as the following: (i) water as a poor solvent, (ii) melt as a θ solvent, and (iii) hexane as a good solvent.

Previously, we reported results of our method for the collapse of short alkane chains in water.[24] The present study differs from the previous one, besides providing important details of the theory, in the following points. First, we employ the mean field (eq 17). Second, although the present work uses the same chain model (RIS), the pentane interaction (between monomers four bonds apart along the chain) is accounted for in a different, computationally more efficient way. In ref 24, this interaction is incorporated in the most direct way by performing Green function iterations with repeat units four bonds long. In the present work, the repeat unit for iteration is just three bonds long, enabling a reduction in the number of coordinates that enter the Green function argument. The pentane interaction is accounted for by an effective rescaling of the rotational potential to increase the persistence length of the chain and match that of a chain with the pentane interaction. As a consequence, the computational costs and memory requirements are reduced by orders of magnitude, enabling treatment of longer molecules. Finally, we consider additional environments in the present study.

An important observation is in place regarding the accuracy of our theory in the case of strongly collapsed chains. Grayce et al.[22,23] have shown that for tangent hard-sphere freely jointed chains in a hard-sphere solvent, there are important limitations of the quality of the pairwise additive solvation potential of the type used here. They demonstrated that three-body effects have an important role and, at least for a melt of hard-sphere short chains, site−site solvation potentials alone cannot reproduce the end-to-end probability distribution function correctly. The use of site−site solvation potentials alone is prone to quantitatively overestimate the effects of the solvent, partly because it ignores the intramolecular screening of the solvent-induced interaction between each pair of sites. With this in mind, we anticipate that the results presented below for alkanes in water are only correct qualitatively. Because the solvent-mediated attraction between its monomers is overestimated for a collapsed chain, we expect the extent of the collapse to be increased, and therefore we do not claim quantitative accuracy of the theory for this system. Nonetheless, the theory provides good qualitative insight in the poor solvent regime as well.

The calculations are performed at $T = 300$ K in water and 415 K in melts and hexane, with experimental data on the coil size in polyethylene melts being available for the latter temperature.[28] The standard density of water was used in the calculations. The density of alkane melt with a given chain length, N, at $T = 415$ K and the atmospheric pressure was determined by interpolation over N between the corresponding densities of decane[35] and polyethylene.[36] The density of liquid hexane at $T = 415$ K was taken from the experimental data[37] available at a pressure of approximately 15 kPa above the saturation pressure for this temperature.

However tempting, the effects of temperature and concentration on the properties of the system are not undertaken in the present study. Instead, we focus on the changes of the conformational properties of the solvated chain in different solvents, and in relevant comparison with the ideal chain. All of the calculations for the solvation properties are carried out in the

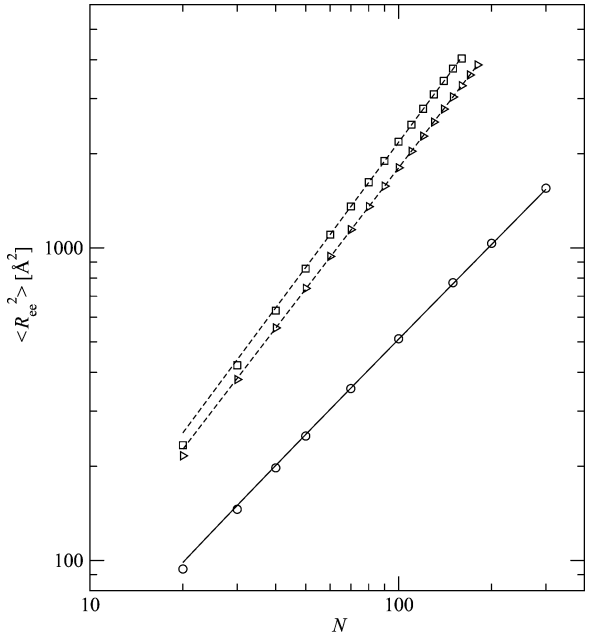

Figure 1. Scaling analysis for the coil size against the number of monomers, N: the freely rotating chain (circles), the ideal RIS chain (triangles), the excluded volume RIS chain (squares), the scaling law fits (dashed lines), and the analytical result (solid line) for the freely rotating chain.[30] The temperature is $T = 415$ K.

limit of infinite dilution. The PY type MIP (eq 5) was used throughout, except where otherwise specified.

Scaling laws of the variation of polymer coil size with respect to the number of monomers are indicative of the quality of solvation in different environments. A well-known fact in polymer science is that for an ideal chain the size of the coil measured by its mean square end-to-end distance or its mean square radius of gyration scales as $R_{ee}^2 \propto N^{\alpha}$ with $\alpha = 1$. End effects are still present for our RIS chain model as well as for real alkane chains. Therefore, the exponent is not exactly 1 even for the longest chain studied here ($N = 200$). To obtain the value 1 exactly, we "stripped" the chain of all the interactions and increased the number of rotational states to mimic the continuum rotational spectrum, thus effectively obtaining a freely rotating chain model. For this model, we found the exponent α to be precisely 1 for $N > 300$. The results of the scaling analysis are shown in Figure 1 as a double logarithmic plot of the mean square end-to-end distance versus chain length. The symbols show the results of our theory, whereas the dashed lines show the scaling law fits (dashed lines) to the data. For the freely rotating chain (circles), the fit practically coincides with the analytical solution (solid line) for this model given, for instance, in Flory's textbook.[30] For the excluded volume chain (in a vacuum) in the infinite chain limit, we expect a scaling exponent of 1.2.[38] Because of chain stiffness at lengths smaller than 200 monomers, our exponent is somewhat larger, 1.33. For the ideal RIS chain with a length up to 200 monomers the exponent is found to be 1.28, appropriately enough less than that for the excluded volume chain. The exponent is expected to approach 1 as the chain length tends to infinity and the ratio of the persistence length to the contour length tends to zero. However, to recover the exact asymptotic scaling laws for the ideal RIS model, one needs to approach chain lengths at least of the order of thousands, which becomes computationally unfeasible at this time.

To test our theory, we approached a simple system studied previously by Monte Carlo simulations and the PRISM theory, namely, a melt of fused-hard-sphere freely rotating chains.[21] In

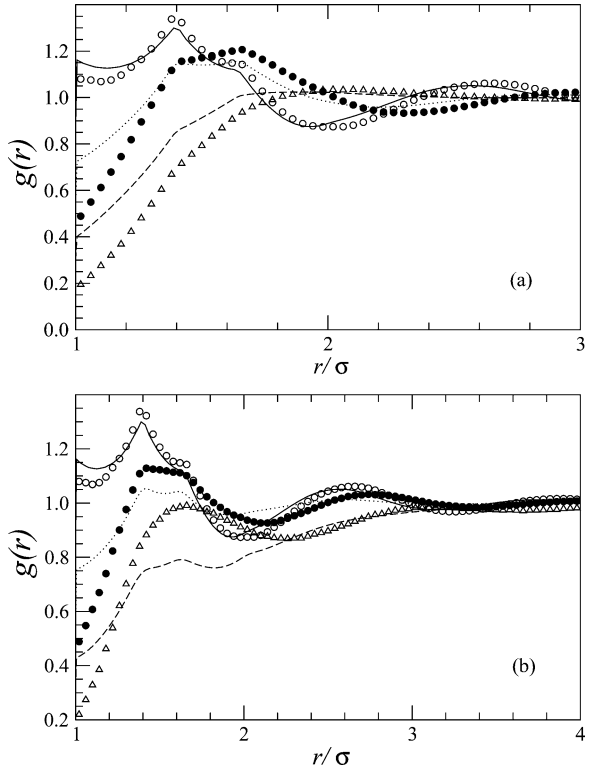

Figure 2. Intermolecular pair correlation functions for a fluid of fused-hard-sphere freely rotating chains obtained in this study as compared to ref 21. Panel a: $N = 4$ and $\rho_m\sigma = 0.25$, 1, and 1.5 in dashed, dotted, and solid lines, respectively, obtained in this study; simulation results[21] for the same parameters are plotted as triangles, filled circles, and empty circles, respectively. Panel b: $\rho_m\sigma = 1.5$ and $N = 4$, 8, and 32 in solid, dotted, and dashed lines, respectively, obtained in this study; simulation results[21] for the same parameters are plotted as empty circles, filled circles, and triangles, respectively.

Figure 2, we present the intermolecular correlation functions for chain lengths $N = 4$, 8, and 32 and volume fractions $\rho_m\sigma = 0.25$, 1, and 1.5 (where σ is the monomer diameter and ρ_m is the number density of monomers) for direct comparison with the results in Figures 1 and 2 of ref 21 for the exact same parameters. The agreement with the shape of g obtained by Monte Carlo simulations (symbols in Figure 2) and by PRISM with the PY closure in ref 21 is satisfactory for all cases.

The use of closure in eq 3a or the HNC closure instead of the PY does not alter the shape of g significantly except for the case $\rho_m\sigma = 0.25$, where a slight increase in the contact value of g is recorded.

The intermolecular pair distribution functions for the various pairs of sites in different systems are presented in Figure 3, where C_p denotes a CH_2 polymer site, C_s denotes a solvent site, and O_w and H_w are for water oxygen and hydrogen, respectively. For nonpolar environments, the correlation peaks and holes are more pronounced and die out slower for a solvent−solvent pair (not shown) than for a solvent−solute pair, but overall the solvation structures are not drastically different around C_p and C_s. The highest correlation peaks form inside the LJ diameter of the polymer site, σ, whereas the major correlation holes fall between σ and 2σ. This behavior is typical of a solvent−solute system with short-ranged interactions, that is, nonpolar molecules. The situation is quite different in water, where the main peak in the solute−solvent pair distribution function is strongly displaced to a location roughly corresponding to the radius of gyration of the polymer. This is due to the formation of "water cages" about a compressed polymer coil, in which water oxygen

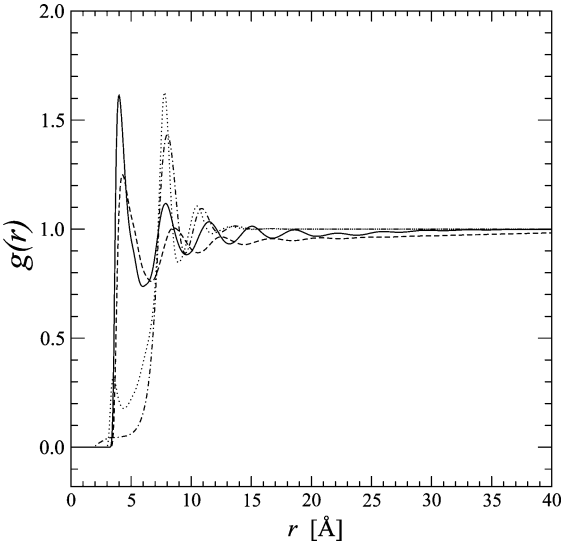

Figure 3. The pair distribution functions for alkanes with chain length $N = 100$ in melts, hexane, and water. The distributions are for the following site pairs: C_p-C_p in melt (solid line), C_p-C_s in hexane (dashed line), C_p-O_w in water (dotted line), and C_p-H_w in water (dash−dotted line). The temperature is $T = 300$ and 415 K for melt and hexane solvent, respectively.

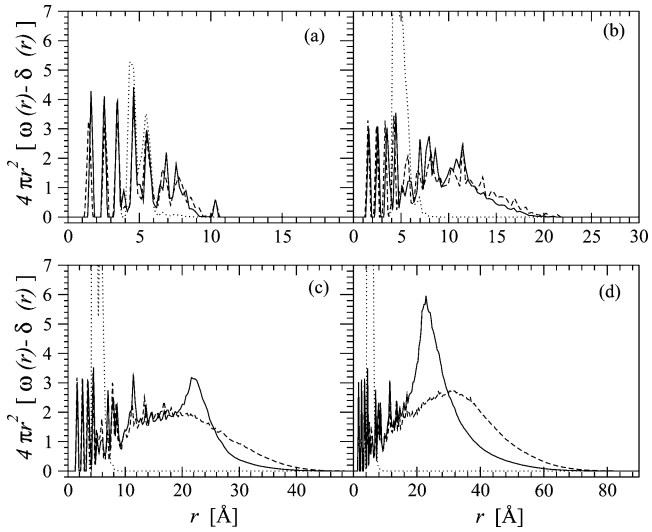

Figure 4. The intramolecular correlation functions for alkane melts with increasing number of monomers $N = 10$, 20, 50, and 100 in parts a−d, respectively. Line types for different environments: solid for melts, dashed for hexane, and dotted for water.

and hydrogen are not likely to penetrate, with the oxygen being slightly more present near the solute site.

A central issue in the solvation of polymer chains is to determine in what fashion and/or to what degree the solvent influences the conformational properties of the molecule. To answer that question, we looked at the shape of the intramolecular correlation function in the absence and then in the presence of the solvent. From that quantity, we can also derive the spatial extent of the chain measured by its radius of gyration, R_g, and the rms end-to-end distance, R_{ee}. The intramolecular correlation functions for chains with various molecular weights in different environments are compared in Figure 4. The expansion of this curve toward greater distances as compared to the ideal chain indicates swelling of the coil, as is observed for hexane solvent, whereas the contraction toward the origin observed for water signals collapse. Note that the contraction of this function for a given chain length does not imply collapse

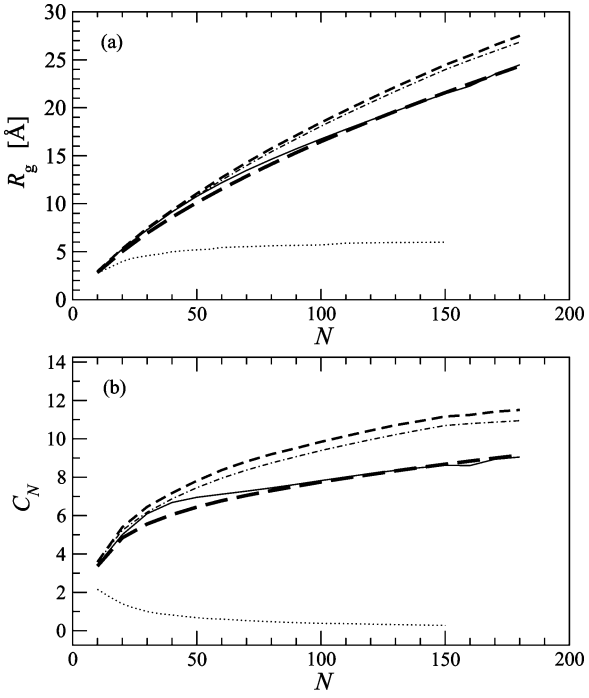

Figure 5. The mean radius of gyration (a) and the characteristic ratio (b) as a function of the chain length for melts (solid lines), hexane solvent (dashed lines), water solvent (dotted lines), ideal chain (long dashed lines), and the excluded volume chain (dash−dotted lines).

into a globular state, but it can instead correspond to a coil with a smaller size. The latter case is obtained for melts, where the polymer behaves like it would in a θ solvent. Only when the contraction with respect to the ideal chain consistently increases for increasing N, one can expect the formation of a globular structure.

Concerning the spatial extent of the polymer coil, we plot in Figure 5 the mean radius of gyration and the characteristic ratio (defined as $C_N = \langle R_{ee}^2 \rangle/(Nb^2)$ as a function of the chain length. The Kuhn length is calculated from the characteristic ratio by $l = Nb^2C_N/L$, where L is the contour length. This also enables quantitative comparison with the experimental data on the dimensions of alkanes. The three distinct regimes of solvation can be observed clearly. For hexane solvent (thick dashed), the curves almost coincide with those of the excluded volume chain and the swelling of the chain with respect to the ideal chain (dash−dotted curve) occurs. For melts (solid curves), the results are just below those for the ideal chain, suggesting the θ condition is realized.[30] In water, the characteristic ratio tends to zero as $N \rightarrow \infty$, whereas the radius of gyration varies insignificantly with N, indicating that the chain is completely collapsed and this is the poor solvent regime.

In Figure 6, we plot the medium-induced potential for the three cases. The shape of this potential varies slightly with N for short chains, and it becomes practically independent of N for chains longer than 20 monomers. The value of the MIP around the contact value at $r = \sigma$ is crucial to the success of solvation of the polymer. The contact value falls below $-2k_BT$ for water solvent, which is much lower than $-0.38k_BT$ for hexane solvent, and $-0.64k_BT$ for melts. Such a difference causes the monomers to stick much closer together in water, inducing collapse of the chain. The presence of the oscillations in the "tail" of the MIP curve for melt and hexane solvation is a consequence of the fact that a polymer site is closely surrounded by sites belonging to other molecules in the environment. For water, the absence of oscillations in the tail

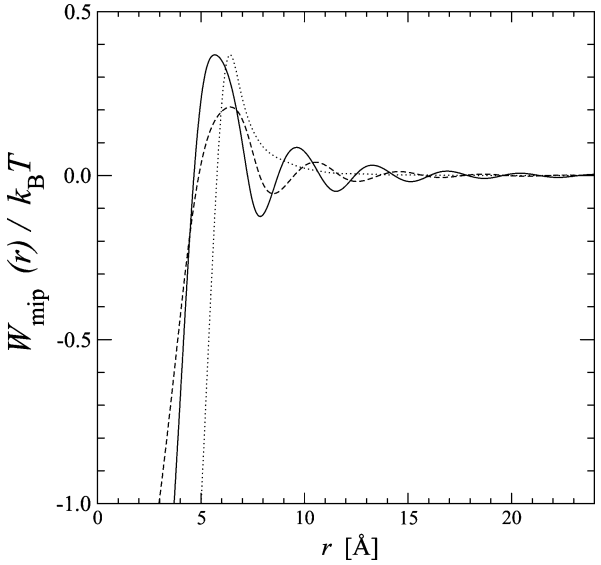

Figure 6. The medium-induced potential of polymer sites in melt (solid line), in hexane (dashed line), and in water (dotted line).

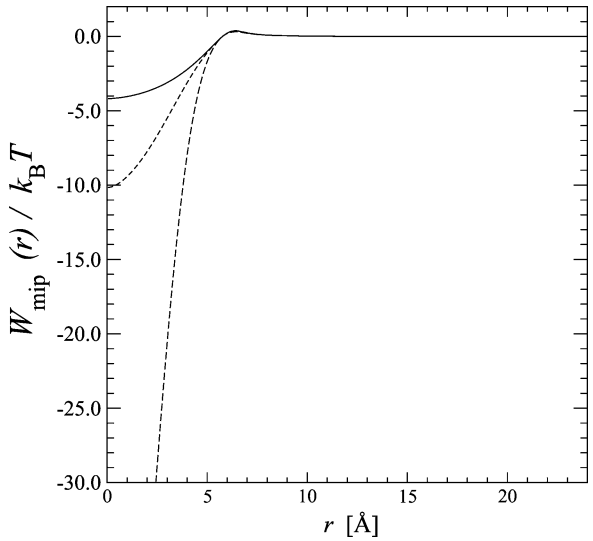

Figure 7. Different forms of the medium-induced potential in water: Percus−Yevick (solid line), Martynov-Sarkisov (dashed line), and HNC (long dashed line).

confirms the fact that a solute site is mainly surrounded by other solute sites immediately.

As we anticipated in the beginning of this section, the extent of the chain collapse in water is overestimated. The degree to which our quantitative results are offset can be analyzed by comparing the dependence of the characteristic ratio on the chain length to the expected scaling law for a compactly collapsed polymer $C_N \propto N^{\alpha}$, with $\alpha = -1/3$. From the results in Figure 5, we extracted an exponent $\alpha = -0.95$, giving a much faster decay of the coil size with increasing N.

We identified a few causes of the deviation from the expected behavior. First, as discussed above, the use of the site−site solvation potentials alone overestimates the effective attraction between monomers in a contracted polymer. Second, because the pentane interaction is only indirectly taken into account in the present Green function implementation, the polymer's short-range steric effect becomes less effective and our predictions tend to overestimate the extent to which neighboring monomers located 4 or 5 bonds apart are allowed to overlap. Furthermore, if we were to use the excluded volume potential in eq 15, then we would get further monomer−monomer attraction because at room temperature, the excluded volume parameter, v_0, is negative. A simple way to compensate for this is to to replace the pair potential in expression 16 for v_0 with its repulsive part only, thus increasing the excluded volume effect. Because for poor solvation we only aim for qualitative results, we left out the term $W^{(ev)}$ in the total potential with no fear of introducing errors. A quantitatively accurate analysis of the hydration cannot be claimed without incorporating many-body effects in the solvation potential,[22,23] which is beyond the scope of this paper.

Another source of variation of the strength of collapse in water resides in the variation of the MIP value in the contact region with the type of closure. The Percus−Yevick type MIP is the least biased in overestimating the magnitude of the MIP around contact, followed by the Martynov-Sarkisov type, and last by the HNC type. One way to compensate for this effect is to ignore or rescale the action of the MIP in the core region at distances where it becomes less than a few $-k_BT$. Note that in our formalism the exclusive action of either the direct MIP or the intramolecular mean field is sufficient to yield collapse of the polymer in water. The difference between medium-induced potentials of different types for water solvent is shown in Figure 7.

For melts and the ideal chain, assuming that the characteristic ratio exhibits a linear asymptotic dependence on the inverse of the chain length, $C_N = C_\infty + const N^{-1}$, we can obtain the value of the characteristic ratio in the infinite chain limit, C_∞, by extrapolation of the curve C_N versus N^{-1} to the limit point $N^{-1} \rightarrow 0$. This enables a comparison with other theoretical and experimental results. The results of this analysis are the following values of C_∞: 9.48 for the ideal chain and 8.92 for melts with the corresponding values of the Kuhn length 17.54 and 16.50 Å, respectively. Our prediction for melt compares reasonably well with the simulation result for melts yielding $C_\infty = 7.9$[29] and with the small-angle neutron scattering on melts yielding $C_\infty = 7.8 \pm 0.4$[44] (earlier intrinsic viscosity measurements[45,46] produced a considerably lower value, 6.7 ± 0.3, which seems to now be obsolete in view of the new measurements and calculations). Recent transfer matrix calculations in the Gibbs ensemble for the continuum rotational potential model in θ solvent[26] yielded $C_\infty = 6.65$, albeit for model parameters taken from the AMBER general force field.[47] This value is thus quite sensitive to the rotational potential and LJ force-field parameters used.

The medium-induced mean fields for the three cases of different solvents are presented in Figure 8. Although one notices the shape of the potentials to vary considerably with N, for chain lengths smaller than 100 monomers, they all become independent of N for chains long enough. The potential for melt (a) is quite similar to the one for hexane solvent (b), except for a small indentation at $r \approx 20$ Å for $N > 50$. This feature is responsible for the smaller coil size as compared to the polymer solvated in hexane. In water (c), the potential well (extending from zero to about 10 Å) responsible for the chain collapse is very similar for all chain lengths and its width is about double the radius of gyration of the polymer chain. The results shown here are for the PY-type MIP. The depth of the well in (c) increases by a factor of about 1.5 for the MS-type MIP and about 2 for the HNC-type.

The intramolecular free energy of alkanes was calculated by using eq 11 for all of the environments. We determined how this quantity is affected by the presence of the solvent by calculating the free-energy difference with respect to the ideal chain. In Figure 9a, we display the values of the free energy per monomer (with respect to the free energy of the ideal chain) for various chain lengths and in different environments. Obvi-

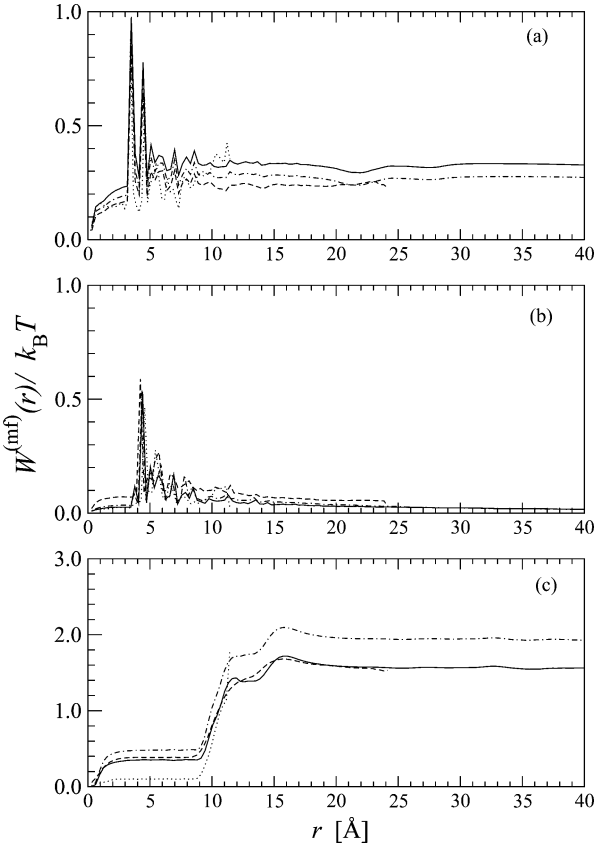

Figure 8. The intramolecular mean field according to eq 17 for alkanes in melt (a), hexane solvent (b), and water (c). Chain lengths: 10, 20, 50, and 100 (dotted, dashed, dash−dotted, and solid lines, respectively).

ously, this analysis singles out the contribution of the medium-induced and excluded-volume potentials to the intramolecular free energy of our model system. We note the nonmonotonic variation of this curve and the trend of this quantity to become N-independent for large values of N. An apparently surprising result is that the intramolecular free-energy values in water do not stand out from the values for the other environments, although the other conformational properties are most drastically affected. This is caused by the fact that, although the entropy of the polymer is greatly reduced, thus increasing the free energy, the internal energy of the chain is decreased considerably due to the low values of the MIP in the contact region. Therefore, the overall effect on the free energy is diminished.

In Figure 9b, we show the variation of the solvation chemical potential per monomer with the chain length for the three environments. The relative positioning of the curves is in accordance with the quality of solvation of the alkanes in the respective environments. Of all of the cases, the curve for hexane solvent has the lowest rate of increase, which is a consequence of the fact that the solvation is very successful in this case. Poor hydration causes the solvation chemical potential for alkanes in water to be much higher than that in hexane solvent and melts, which reflects the increasing energy cost of building water cages of increasing size in bulk water.

In Figure 10, we plot the partial molar volume (PMV) per monomer as a function of chain length. The PMV of alkanes in water is the lowest as a consequence of the fact that the polymer is compressed by the surrounding water molecules to the highest degree. The PMV becomes constant for $N > 20$, which corresponds to the length beyond which the chain can form a compact globule (when maximum compression is achieved). In hexane solvent, the creation of any vacuum cavities

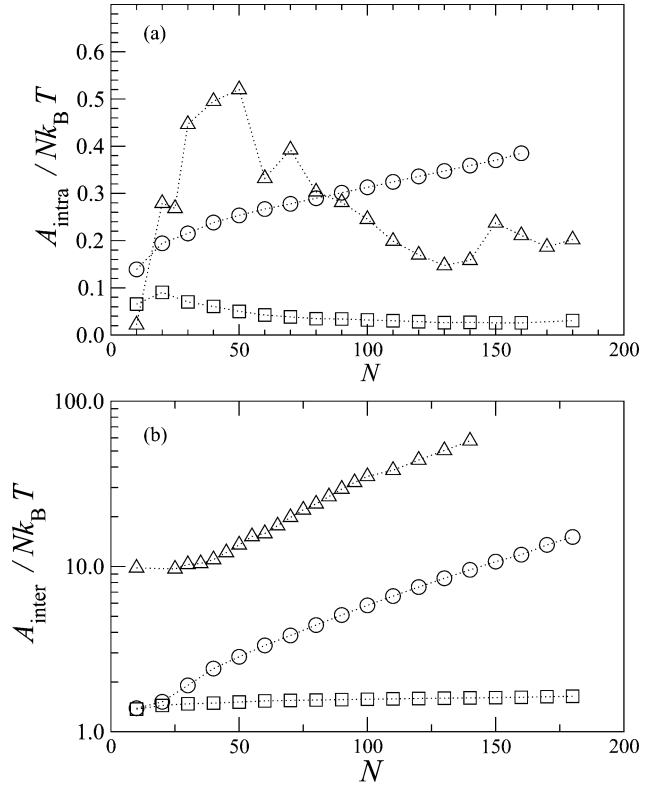

Figure 9. The intramolecular free energy per monomer with respect to that of the ideal chain (a) and the solvation free energy per monomer (b) as a function of the chain length for melts (circles), hexane solvent (squares), and water solvent (triangles).

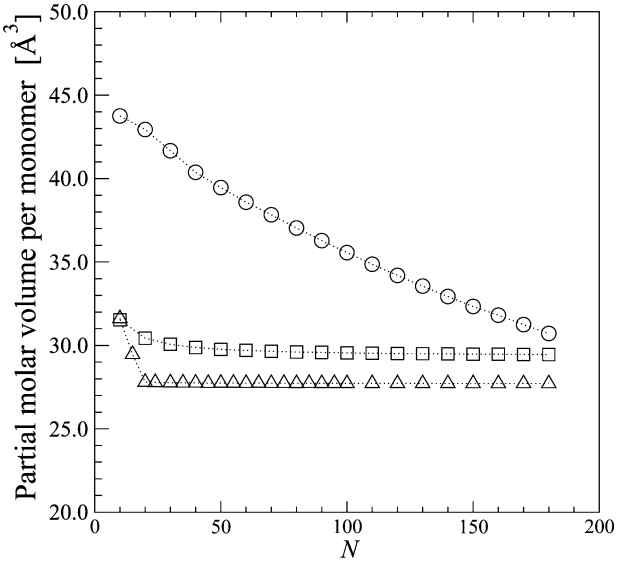

Figure 10. The partial molar volume per monomer as a function of the chain length for melts (circles), hexane solvent (squares), and water solvent (triangles).

is less costly and the chain is swollen. Finally, in melts, we obtain a strong variation of the PMV with N because the melt density varies with chain length.

4. Concluding Remarks and Outlook

We developed a new method for calculating the properties of solute−solvent systems. The intramolecular correlation functions for flexible polymer molecules and the intermolecular correlation functions are self-consistently calculated via a powerful combination of the polymer's Green function formal-

ism with the PRISM theory. We have analyzed the conformational changes of alkane molecules in melt and in different solvents. The main merit of the present formalism is that it recovers, to an extent exceeding the qualitative level, the three regimes of solvation of alkane chains: good solvation in hexane accompanied by the swelling of the coil, poor solvation in water accompanied by the chain collapse and the formation of a globule, and finally θ condition in melts where the chain behaves more or less as an ideal one.

Overall, our method yields good agreement with the expected behavior and other theoretical and experimental results. The closure (eq 3a) used for the first time for solutions of flexible polymeric chains proves to be appropriate for such systems. We obtain reasonable predictions of the chain size in melt and good solvent for chain lengths for which end effects are still present. The solvation free energy is an indicator of the success of the polymer's solvation; its values are highest in water (poor solvation) and lowest in hexane (good solvation). In hexane solvent, the values of both the conformational and solvation free energy per monomer level off for chain lengths much smaller than 200. This is not the case in the other two environments where, up to the longest chains studied here, there are still strong variations of these quantities. A practical consequence is that in order to make predictions of the solvation energy of a polymer in a good solvent one needs to approach only relatively short chains.

Our results for the hydration of alkanes are only correct qualitatively, with the quantitative aspect being marked by an overestimation of the solvent-mediated attraction between pairs of collapsed monomers. An appropriate solvation potential for this case would entail accounting in a rigorous way for the intramolecular screening of the site−site MIP as well as the folding configurations of adjacent polymer segments compatible with the chain architecture. Although this regime requires the incorporation of many-body interactions in both the solvation potential and the Green function approach, it is an issue beyond the scope of this paper.

Although the method is applied here to homopolymers, it can be extended to copolymers with any given size and chemical structure without any conceptual changes. In that case, the formalism will be adapted to incorporate variable bond lengths, bond angles, and rotational potential. Furthermore, within the PRISM formalism with the closure used here is it possible to treat polar solvent and solute molecules. A matter worth a detailed investigation would be to see how far such a formalism based on the reduction of many-body effects to two-body interactions would successfully calculate the properties of such complex systems. This task will be undertaken in future studies.

Acknowledgment. This work is supported by the National Research Council of Canada. We thank Professor Arun Yethiraj for providing the Monte Carlo simulation data on freely rotating chains.

References and Notes

(1) Chandler, D.; Andersen, H. C. *J. Chem. Phys.* **1972**, *57*, 1930.
(2) Singer, S. J.; Chandler, D. *Mol. Phys.* **1985**, *55*, 621.
(3) Schweizer, K. S.; Curro, J. G. *Phys. Rev. Lett.* **1987**, *58*, 246.
(4) (a) Schweizer, K. S.; Curro, J. G. *Macromolecules* **1988**, *21*, 3070. (b) Schweizer, K. S.; Curro, J. G. *Macromolecules* **1988**, *21*, 3082.
(5) Schweizer, K. S.; Curro, J. G. *J. Chem. Phys.* **1989**, *91*, 5059.
(6) Schweizer, K. S.; Honnell, K. G.; Curro, J. G. *J. Chem. Phys.* **1992**, *96*, 3211.
(7) Melenkevitz, J.; Curro, J. G. *J. Chem. Phys.* **1993**, *99*, 5571.
(8) Melenkevitz, J.; Schweizer, K. S.; Curro, J. G. *Macromolecules* **1993**, *26*, 6190.
(9) Grayce, C. J.; Yethiraj, A.; Schweizer, K. S. *J. Chem. Phys.* **1994**, *100*, 6857.
(10) Donley, J. P.; Rajasekaran, J. J.; McCoy, J. D.; Curro, J. G. *J. Chem. Phys.* **1995**, *103*, 5061.
(11) Munakata, T.; Yoshida, S.; Hirata, F. *Phys. Rev. E* **1996**, *54*, 3687.
(12) Sumi, T.; Hirata, F. *J. Chem. Phys.* **2003**, *118*, 2431.
(13) Yethiraj, A.; Fynewever, H.; Shew, C. Y. *J. Chem. Phys.* **2001**, *114*, 4323.
(14) Frischknecht, A. L.; Weinhold, J. D.; Salinger, A. G.; Curro, J. G.; Douglas Frink, J. D. *J. Chem. Phys.* **2002**, *117*, 10385.
(15) Frischknecht, A. L.; Weinhold, J. D.; Salinger, A. G.; Curro, J. G.; Douglas Frink, J. D. *J. Chem. Phys.* **2002**, *117*, 10398.
(16) Yethiraj, A.; Hall, C. K. *J. Chem. Phys.* **1992**, *96*, 797.
(17) Yethiraj, A. *J. Chem. Phys.* **1994**, *101*, 9104.
(18) Mendez, S.; Curro, J. G. *Macromolecules* **1980**, *13*, 2004.
(19) Yethiraj, A. *J. Chem. Phys.* **1998**, *108*, 1184.
(20) Shew, C.-Y.; Yethiraj, A. *J. Chem. Phys.* **1997**, *106*, 5706.
(21) Yethiraj, A. *J. Chem. Phys.* **1995**, *102*, 6874.
(22) Grayce, J. G. *J. Chem. Phys.* **1997**, *106*, 5171.
(23) Grayce, J. G.; de Pablo, J. J. *J. Chem. Phys.* **1994**, *101*, 6013.
(24) Livadaru, L.; Kovalenko, A. *J. Chem. Phys.* **2004**, *121*, 4449.
(25) Leach, A. R. *Molecular Modelling: Principles and Applications*; Prentice Hall, London, 2001.
(26) Livadaru, L.; Kreuzer, H. J. *Phys. Chem. Chem. Phys.* **2004**, *6*, 3872.
(27) Mayo, S. L.; Olafson, B. D.; Godard, W. A., III *J. Phys. Chem.* **1990**, *94*, 8897.
(28) Boothroyd, A. T.; Rennie, A. R.; Boothroyd, C. B. *Europhys. Lett.* **1991**, *15*, 715.
(29) Han, J.; Jaffe, R. L.; Yoon, D. Y. *Macromolecules* **1997**, *30*, 7245.
(30) Flory, P. J. *Statistical Mechanics of Chain Molecules*; Hanser Verlag: München, Germany, **1989**.
(31) Kovalenko, A.; Hirata, F. *J. Chem. Phys.* **1999**, *110*, 10095.
(32) Kovalenko, A.; Hirata, F. *J. Theor. Comput. Chem.* **2002**, *1*, 381.
(33) Livadaru, L.; Netz, R. R.; Kreuzer, H. J. *Macromolecules* **2003**, *36*, 3732.
(34) Livadaru, L.; Netz, R. R.; Kreuzer, H. J. *J. Chem. Phys.* **2003**, *118*, 1404.
(35) Brandrup, J.; Immergut, E. H. *Polymer Handbook*; Wiley: New York, 1989.
(36) Olabisi, O.; Simha, R. *Macromolecules* **1975**, *8*, 206.
(37) Beg, S. A.; Tukur, N. M.; Al-Harbi, D. K.; Hamad, E. Z. *J. Chem. Eng. Data* **1993**, *38*, 461.
(38) Doi, M.; Edwards, S. F. *The Theory of Polymer Dynamics*; Oxford University Press: New York, 1994.
(39) Lifson, S. *J. Chem. Phys.* **1959**, *30*, 964.
(40) Nagai, K. J. *J. Chem. Phys.* **1959**, *31*, 1169.
(41) Birshtein, T. M.; Ptitsyn, O. B. *Zh. Tekh. Fiz.* **1959**, *29*, 523.
(42) Volkenstein, M. V. *Configurational Statistics of Polymeric Chains*; Interscience: New York, 1963.
(43) Kovalenko, A.; Ten-No, S.; Hirata, F. *J. Comput. Chem.* **1999**, *20*, 928.
(44) Horton, J. C.; Squires, G. L.; Boothroyd, T.; Fetters, L. J.; Rennie, A. R.; Glinka, C. J.; Robinson, R. A. *Macromolecules* **1989**, *22*, 681.
(45) Chiang, R. *J. Chem. Phys.* **1966**, *70*, 2348.
(46) Stacy, C. J.; Arnett, R. L. *J. Chem. Phys.* **1965**, *69*, 3109.
(47) Cornell, W. D.; Cieplak, P.; Bayly, C. I.; Gould, I. R.; Merz, K. M.; Ferguson, D. M.; Spellmeyer, D. C.; Fox, T.; Caldwell, J. W.; Kollman, P. A. *J. Am. Chem. Soc.* **1995**, *117*, 5179.